THE JOURNAL OF BIOLOGICAL CHEMISTRY VOL. 283, NO. 29, pp. 19948–19956, July 18, 2008

Proliferation *Versus* Migration in Platelet-derived Growth Factor Signaling

*THE KEY ROLE OF ENDOCYTOSIS**

Received for publication, November 16, 2007, and in revised form, April 11, 2008 Published, JBC Papers in Press, May 21, 2008, DOI 10.1074/jbc.M709428200

Alina De Donatis[‡], Giusy Comito[‡], Francesca Buricchi[‡], Maria C. Vinci[§], Astrid Parenti[§], Anna Caselli[‡], Guido Camici[‡], Giampaolo Manao[‡], Giampietro Ramponi[‡], and Paolo Cirri[‡1]

From the [‡]Dipartimento di Scienze Biochimiche and the [§]Dipartimento di Farmacologia Preclinica e Clinica, Università degli Studi di Firenze, Viale Morgagni 50, 50134 Firenze, Italy

It is common knowledge that platelet-derived growth factor (PDGF) is a critical regulator of mesenchymal cell migration and proliferation. Nevertheless, these two cellular responses are mutually exclusive. To solve this apparent contradiction, we studied the behavior of NIH3T3 fibroblasts in response to increasing concentrations of PDGF. We found that there is strong cell proliferation induction only with PDGF concentrations >5 ng/ml, whereas the cell migration response arises starting from 1 ng/ml and is negligible at higher PDGF concentrations. According to these phenotypic evidences, our data indicate that cells display a differential activation of the main signaling pathways in response to PDGF as a function of the stimulation dose. At low PDGF concentrations, there is maximal activation of signaling pathways linked to cytoskeleton rearrangement needed for cell motility, whereas high PDGF concentrations activate pathways linked to mitogenesis induction. Our results suggest a mechanism by which cells switch from a migrating to a proliferating phenotype sensing the increasing gradient of PDGF. In addition, we propose that the cell decision to proliferate or migrate relies on different endocytotic routes of the PDGF receptor in response to different PDGF concentrations.

Receptor tyrosine kinases regulate many aspects of cellular physiology such as proliferation, survival, migration, and differentiation (1), transducing and integrating extracellular signaling inputs coming from soluble as well as insoluble molecules. In particular, it is well known that platelet-derived growth factor (PDGF),[2] interacting with its receptor on the surface of target cells, induces and regulates many physiologic and pathologic processes such as wound healing and tissue repair, tissue development (*i.e.* neural/oligodendrocytic and hematopoietic development and angiogenesis) and organogenesis, and cancer progression and metastasis (2). PDGF exerts its multifaceted functions by binding to the PDGF receptor (PDGFR), which dimerizes, activates its intrinsic catalytic activity, and undergoes autophosphorylation on >10 specific tyrosines that serve as docking sites for intracellular signaling molecules harboring the SH2 (Src homology 2) or protein tyrosine-binding domain (3, 4), such as phosphatidylinositol 3-kinase (PI3K), phospholipase Cγ, the Src family of tyrosine kinases, the SHP-2 tyrosine phosphatase, and Ras GTPase-activating protein, as well as adaptor molecules such as Grb2, Shc, Nck, Grb7, and Crk and STAT (signal transducer and activator of transcription) proteins. It has been largely reported that the activation of these multiple pathways leads ultimately to various kinds of cellular responses (*i.e.* cell proliferation, survival, migration, and differentiation) (4–6). In this work, we studied the mechanism by which PDGF signaling, transduced by the same intracellular molecules, on the same cell type (mouse NIH3T3 fibroblasts) is able to induce two radically different phenotypic outputs: migration and proliferation. What is the molecular basis of the cell decision to proliferate or to migrate sensing the same kind of stimulus? Our working hypothesis is that any single cell chooses to proliferate or migrate depending on the PDGF concentration in the environment. There are many physiologic and pathologic situations in which a growth factor gradient can be formed, *e.g.* during development, wound healing, and angiogenesis, as well as in cancer growth. In such conditions, target cells more distant from the gradient source sense a relatively low PDGF concentration, and their phenotypic response consists of directional cell migration along the gradient. When migrating cells arrive at a point at which the PDGF concentration reaches a precise threshold, they switch from a migrating phenotype to a proliferating one, leading, in the case of wound healing, to efficient tissue repair.

Our experimental results essentially confirm this model. Moreover, we propose that differential routes of PDGFR endocytosis as a function of PDGF concentrations play a fundamental role in determining the cellular phenotypic output. Low PDGF doses induce clathrin-mediated endocytosis (CME), which is not sufficient *per se* to elicit cell proliferation. In this condition, PDGFR remains prevalently on the cell surface, acting essentially as a sensor. At high PDGF concentrations, PDGFR internalization shifts, at least partially, toward a different kind of mechanism: raft/caveolin-mediated endocytosis

* This work was supported in part by FIRB 2001 Grant RBNE01KJHT_003 (to G. C.) and the Ente Cassa di Risparmio di Firenze. The costs of publication of this article were defrayed in part by the payment of page charges. This article must therefore be hereby marked "*advertisement*" in accordance with 18 U.S.C. Section 1734 solely to indicate this fact.

[1] To whom correspondence should be addressed. Tel.: 39-55-459-8302; Fax: 39-55-459-8905; E-mail: paolo.cirri@unifi.it.

[2] The abbreviations used are: PDGF, platelet-derived growth factor; PDGFR, PDGF receptor; PI3K, phosphatidylinositol 3-kinase; CME, clathrin-mediated endocytosis; RME, raft/caveolin-mediated endocytosis; ERK, extracellular signal-regulated kinase; RIPA, radioimmune precipitation assay; PAK, p21-activated kinase; GST, glutathione *S*-transferase; siRNA, small interfering RNA; FAK, focal adhesion kinase; EGFR, epidermal growth factor receptor.

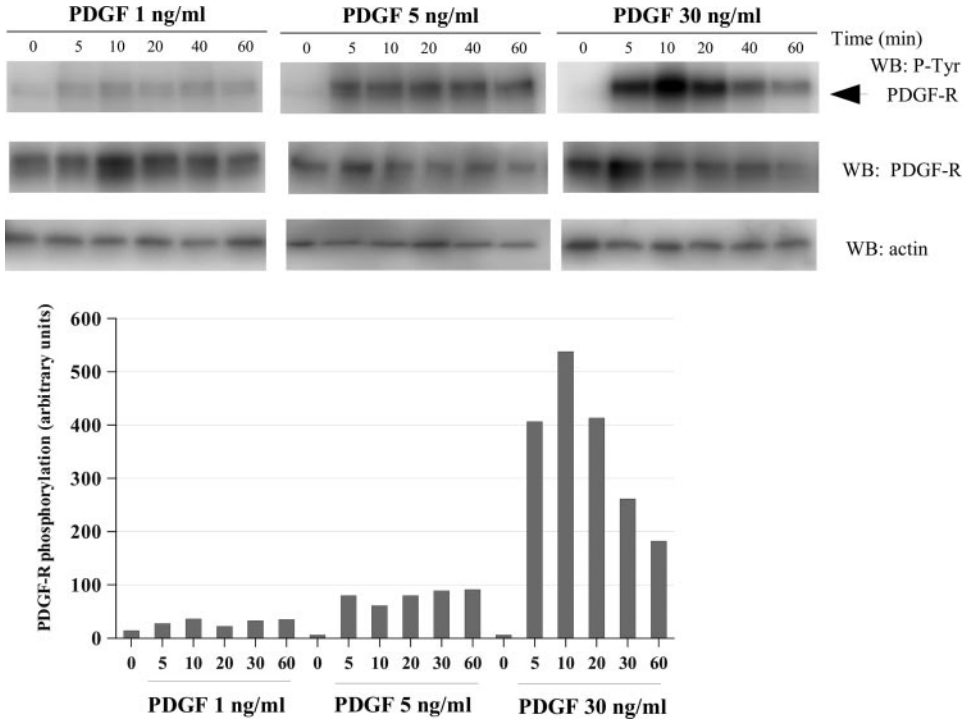

FIGURE 1. **Dose- and time-dependent PDGFR phosphorylation.** NIH3T3 cells were serum-starved for 24 h; stimulated with 1, 5, and 30 ng/ml PDGF for the indicated times; and then lysed with SDS sample buffer. Lysates were used for Western blot (*WB*) analysis. The membranes were treated with anti-phosphotyrosine antibodies, with anti-PDGFR antibodies, and with anti-actin antibodies for normalization. The histogram shows the densitometric analysis of phosphorylated PDGFR normalized with respect to actin. The data are representative of five independent experiments.

(RME). In the latter case, PDGFR is able to start the mitotic process and then undergoes proteasomal degradation.

EXPERIMENTAL PROCEDURES

Materials—Unless specified otherwise, all reagents were obtained from Sigma. Filipin was from Fluka. Mouse NIH3T3 fibroblasts were purchased from ECACC. Human recombinant PDGF-BB was from PeproTech. The enhanced chemiluminescence kit was from Millipore. Rac1 and ROCK (G protein Rho-associated kinase) inhibitors (NSC23766 and Y-27632) were from Calbiochem. All antibodies were from Santa Cruz Biotechnology, except anti-phospho-ERK antibody, which was from New England Biolabs, and anti-phosphotyrosine antibody (4G10), which was from Upstate Biotechnology. BCA protein assay reagent and Sulfo-NHS-SS-Biotin were from Pierce. Rho assay reagent (rhotekin Rho-binding domain-agarose) was from Upstate Biotechnology. Lipofectamine was from Invitrogen. RNA interference oligonucleotides for dynamin-2 were from Qiagen Inc.

Cell Culture—NIH3T3 cells were routinely cultured in Dulbecco's modified Eagle's medium supplemented with 10% bovine calf serum in a 5% CO_2 humidified atmosphere.

Crystal Violet Staining—2×10^4 NIH3T3 cells were seeded onto 24-multiwell plates and serum-starved for 24 h before receiving the reported dose of PDGF for 24 and 48 h. Fresh growth factor was added daily. Cell growth was stopped by removing the medium and adding a 0.5% crystal violet solution in 20% methanol. After 5 min of staining, the fixed cells were washed with phosphate-buffered saline and solubilized with 0.1 M sodium citrate, pH 4.2 (200 μl/well). The absorbance at 595 nm was evaluated using a microplate reader.

Biochemical Analysis—1×10^6 cells were seeded onto 10-cm plates in Dulbecco's modified Eagle's medium supplemented with 10% bovine calf serum. Cells were serum-starved for 24 h before receiving PDGF. Pharmacologic inhibitors (12.5 mg/ml nystatin plus 0.25 mg/ml filipin) were added to the cells for 1 h at 37 °C before stimulation. Cells were then lysed for 20 min on ice in 0.5 ml of complete radioimmune precipitation assay (RIPA) buffer (50 mM Tris-HCl, pH 7.5, 150 mM NaCl, 1% Nonidet P-40, 0.1% SDS, 0.5% sodium deoxycholate, 2 mM EGTA, 1 mM sodium orthovanadate, 1 mM phenylmethanesulfonyl fluoride, 10 μg/ml aprotinin, and 10 μg/ml leupeptin). Lysates were clarified by centrifugation and immunoprecipitated for 4 h at 4 °C with 0.1 μg of the specific antibodies. Immune complexes were collected on protein A-Sepharose (Sigma), separated by SDS-PAGE, and transferred onto polyvinylidene difluoride membrane (Millipore). Immunoblots were incubated in 1% bovine serum albumin, 10 mM Tris-HCl, pH 7.5, 1 mM EDTA, and 0.05% Tween 20 for 1 h at room temperature; probed first with specific antibodies and then with secondary antibodies conjugated with horseradish peroxidase; washed; and developed with the enhanced chemiluminescence kit. Chemiluminescence was detected using the Gel Logic 2200 imaging system (Eastman Kodak Co.). Kodak MI software was used to perform the quantitative analysis of the spots.

Rho and Rac pulldown assays were performed by treating the cells as described above. In complete RIPA buffer, cell lysates were added to 10 μl of rhotekin Rho-binding domain-agarose (Rho) or PAK-CRIB-GST-agarose (Rac). Samples was kept for 1 h at 4 °C, washed twice with 1 ml of complete RIPA buffer, denatured with 15 μl of SDS sample buffer, and subjected to SDS-PAGE and Western blot analysis as described above.

Small Interfering RNA (siRNA) Transfection—Transfections were performed using Lipofectamine. The target sequences in the mouse dynamin-2 gene were CTGCCTCTGTATATC-CTATTA and CTGGCTCAAGTTGTATATATA. Control siRNA had three mutations in the sequence of dynamin-2 siRNA. Cells were used for the experiments after 3 days of transfection.

Two-dimensional Migration and Proliferation Assay of Adherent Cells in Culture—Two-dimensional lateral sheet migration and proliferation of adherent cells in culture were evaluated using a silicon template fencing technique as reported previously (7). Briefly, cells in 10% bovine calf serum

were seeded onto a rectangular silicon gasket inserted inside the wells of 6-well cell culture dishes and allowed to reach confluence. The gasket was then removed; confluent cell monolayers were washed with medium; and the four edges of the rectangular cell monolayer were marked with a scalpel on the outside of the tissue culture dish to define the starting line of cell progression. PDGF (in 0% bovine calf serum medium) was added, and the experiment was stopped after 24 h. Cell migration was quantified by (*a*) measuring microscopically the distance of migrated cells from the starting lines to the migration front (the farthest cells) with the aid of an ocular grid (225 × 225 μm = 1 grid unit) and (*b*) counting the total number of cells in each grid unit according to the method described elsewhere (7).

PDGFR Internalization Assay—PDGFR internalization was determined according to Roberts *et al.* (8). Briefly, cells were serum-starved for 24 h and then labeled with 0.2 mg/ml Sulfo-NHS-SS-Biotin in phosphate-buffered saline for 45 min on ice. Cell were incubated for 10 min on ice with 50 mM Tris, pH 8.0, and 100 mM NaCl to quench the unbound biotin. Cell were prewarmed at 37 °C for 5 min and then stimulated with 2 or 30 ng/ml PDGF for the indicated times. Biotin was removed from proteins remaining at the cell surface by incubation with a solution of 20 mM sodium 2-mercaptoethanesulfonate in 50 mM Tris, pH 8.6, and 100 mM NaCl for 2 min on ice. Sodium 2-mercaptoethanesulfonate was inactivated by adding a solution of 20 mM iodoacetic acid in phosphate-buffered saline for 10 min on ice, and the cells were then lysed as described above. Lysates were clarified by centrifugation at 10,000 × *g* for 20 min, and the biotinylated proteins of the supernatant were precipitated with streptavidin-agarose resin.

Cytofluorometric Analysis—10^5 NIH3T3 cells were seeded onto 60-mm dishes, and after 24 h of starvation, they were stimulated with 0, 1, 5, or 30 ng/ml PDGF. After 19 h, cells were rinsed twice with cold phosphate-buffered saline and lysed in 0.6 ml of 50 mg/liter propidium iodide hypotonic solution. Sample analysis was performed in a BD Biosciences FACS-Canto using FACSDiva and ModFit cell analysis software.

Data Analysis—The results shown are from at least three separate experiments performed in duplicate. Data are expressed as the means ± S.E. Statistical analysis of the data was performed by Student's *t* test. *p* values <0.05 were considered significant.

RESULTS

PDGF Dose-dependent Phenotypic Response of NIH3T3 Cells—The time course of PDGFR phosphorylation in cells stimulated with 30 ng/ml PDGF (Fig. 1) reached a maximum after 10 min and rapidly declined thereafter. The time course of PDGFR phosphorylation at both 5 and 1 ng/ml was lower, as expected, compared with 30 ng/ml PDGF, but interestingly, the phosphorylation signal was more persistent (Fig. 1). The proliferative effect of PDGF concentrations on NIH3T3 cells (Fig. 2*A*) was a function of stimulation dose. In particular, cytofluorometric analysis of cells after 19 h of stimulation (Fig. 2*B*) with various PDGF concentrations demonstrated that doses <2 ng/ml did not elicit S phase cell entry, whereas at concentrations >5 ng/ml, cells entered S phase proportionally to the stimulation dose.

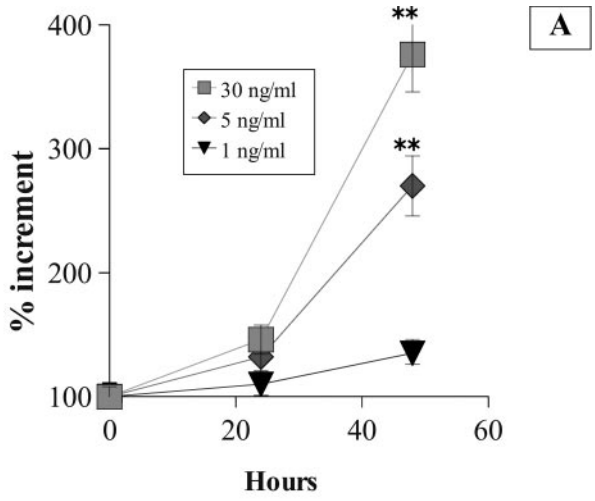

B

PDGF (ng/ml)	0	0.5	1	2	5	10	30
% G_0	94.1	96.1	94.9	93.8	43.7	33.4	22.0
% S	5.4	3.0	4.4	5.2	**36.8**	**43.3**	**52.8**
% G_2/M	0.5	0.9	0.7	1.0	19.5	23.3	25.2

FIGURE 2. **Dose-dependent PDGF-induced cell growth.** *A*, analysis of cell growth rate. 5×10^5 NIH3T3 cells were seeded onto 10-mm dishes and stimulated with the indicated PDGF concentrations 24 h after starvation. After 24 and 48 h of stimulation, the cells were fixed with 0.5% crystal violet solution in 20% methanol. Cell growth was evaluated by measuring absorbance at 595 nm as described under "Materials and Methods." $n = 5$ in duplicate. **, $p < 0.001$ *versus* 1 ng/ml PDGF. *B*, cytofluorometric analysis. 5×10^5 NIH3T3 cells were seeded onto 10-mm dishes and stimulated with the indicated PDGF concentrations 24 h after starvation. After 19 h, cells were lysed in 1 ml of propidium iodide solution and analyzed as described under "Materials and Methods." The data are representative of three independent experiments.

We next examined the dose-dependent effect of PDGF on NIH3T3 cell migration. First, we used a wound healing assay (Fig. 3*A*), which demonstrated that low doses of PDGF (1 or 2 ng/ml), at which there was no cell proliferation (Fig. 2*B*), caused migration, whereas higher doses of PDGF (5 or 30 ng/ml) showed a repair of the "wound" that was probably due to both cell proliferation and migration. To better dissect this aspect, we quantified the cell migration both by measuring microscopically the distance of the migrated cells from the starting lines to the migration front and by counting the total number of cells in each grid unit (see "Materials and Methods"). Fig. 3 (*A* and *B*) shows that 1 ng/ml PDGF was better able to induce cell migration compared with higher doses considering the cell number in the function of the distance traveled. In conclusion, low PDGF concentrations (1–2 ng/ml) are able to induce cell migration but not cell proliferation, whereas at high PDGF doses (5–30 ng/ml), cell proliferation induction prevails. Hence, increasing PDGF doses are able to induce a progressive shift from the migrating to proliferating phenotype in NIH3T3 cells.

PDGF Dose-dependent Differential Activation of Intracellular Signaling Pathways—PDGFR phosphorylation increases fairly linearly with PDGF dose stimulation (see Fig. 1), but the changes in phenotypic outcome are not linear at all. In fact, we

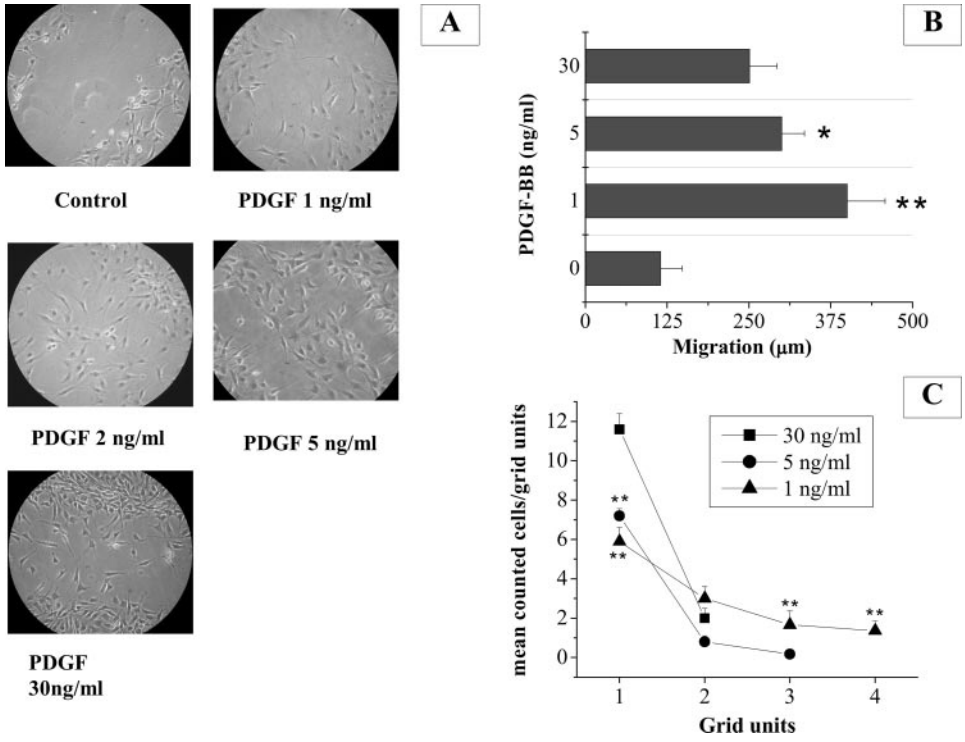

FIGURE 3. *A*, NIH3T3 cells stimulated with PDGF were subjected to wound healing assay. 24 h after starvation, a wound was produced on the cell layer using a pipette tip. The cells were then stimulated with the indicated concentrations of PDGF. Wound repair after 24 of stimulation was observed under a microscope. The data are representative of three independent experiments. *B*, PDGF induces cell migration. Shown is the effect of PDGF (1–30 ng/ml) on the migration of adherent NIH3T3 cells in culture. *C*, the sprouting of cells is expressed as the distance traveled (in μm) by cells from the starting line. The distance was calculated using an ocular grid (see "Materials and Methods:). In *B*, the data are the means $\pm$ S.E. of cells counted in each grid (grid unit = 225 $\times$ 225 μm) in response to PDGF. $n = 3$ in duplicate. *, $p < 0.005$ *versus* 30 ng/ml PDGF; **, $p < 0.001$ *versus* 30 ng/ml PDGF.

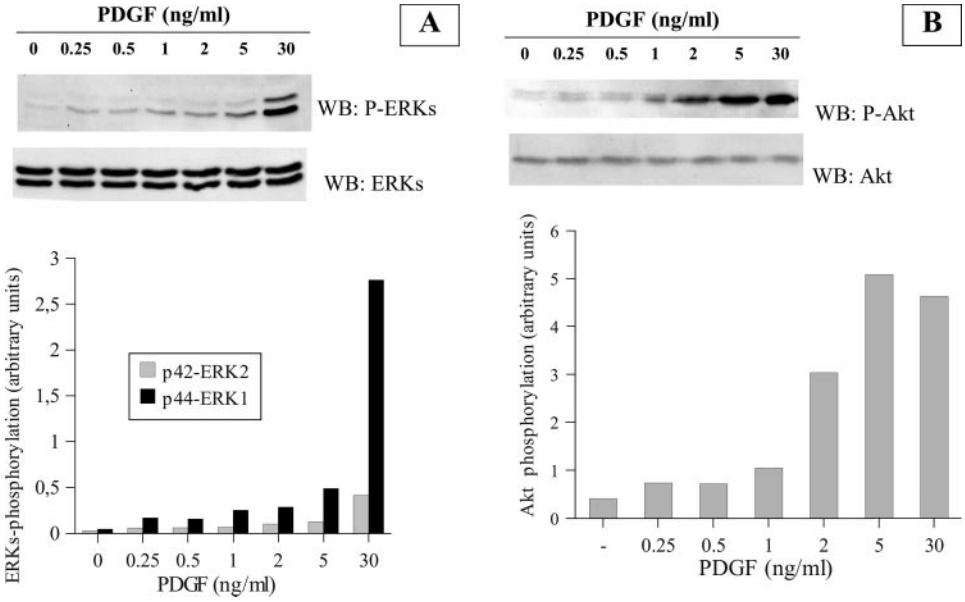

FIGURE 4. *A*, determination of ERK phosphorylation after PDGFR stimulation. NIH3T3 cells were serum-starved for 24 h and then stimulated with PDGF at the indicated concentrations for 5 min, followed by Western blot analysis (*WB*). The membrane was treated with anti-phospho-ERK antibodies and then stripped and reprobed with anti-ERK antibodies. The values in the histogram represent the ratio between the values obtained by densitometric analysis of the bands. The data are representative of three independent experiments. *B*, determination of Akt phosphorylation after PDGFR stimulation. NIH3T3 cells were serum-starved for 24 h and then stimulated for 5 min with PDGF at the indicated concentrations. Lysates were used for Western blot analysis with anti-phospho-Akt antibodies. The membrane was stripped and reprobed with anti-Akt antibodies. The values in the histogram represent the ratio between the values obtained by densitometric analysis of the bands. The data are representative of three independent experiments.

observed a drastic change in the cellular program as a function of PDGF concentration. We chose to study the dose-dependent intracellular signaling of PDGF, focusing in particular on pathways such as those initiated by PI3K and Ras activation as prototypes of proliferating and anti-apoptotic mediators of PDGF stimulation and by Rho, Rac, and focal adhesion kinase (FAK) activation as prototypes of pathways involved in cytoskeleton remodeling and cell migration.

Ras/ERK cascade activation due to growth factor receptor stimulation is one of the most important signaling pathways promoting cellular division (9, 10). The dose-dependent activation of ERKs (Fig. 4*A*), as expected, paralleled that of PDGFR phosphorylation according to the fact that a pathway heavily involved in cell cycle progression is more active at high PDGF concentrations (5 and 30 ng/ml), at which we observed a strong mitosis induction.

The other mitosis-related pathway that we examined was PI3K/Akt (Fig. 4*B*). PI3K activation has a major role in activating growth factor-stimulated cell cycle progression (11–14). Surprisingly, the dose-dependent activation of PI3K/Akt was not superimposable on that of PDGFR activation (Fig. 1*A*). In fact, the Akt phosphorylation level began to increase at a 1–2 ng/ml PDGF stimulation dose, at which there was no proliferation induction. One possible explanation may be that Akt activation is important not only in cell proliferation but also serves in anti-apoptotic signaling (15), and hence, this pathway needs to be active also when cells are not proliferating (*i.e.* low PDGF concentration).

FAK is a tyrosine kinase (16-19) localized to the extracellular matrix/integrin junction and whose function, stimulated by various extracellular signals such as growth factors and extracellular matrix/integrin engagement, is to promote the rearrangement of focal adhesion in cell motility regulation. PDGF

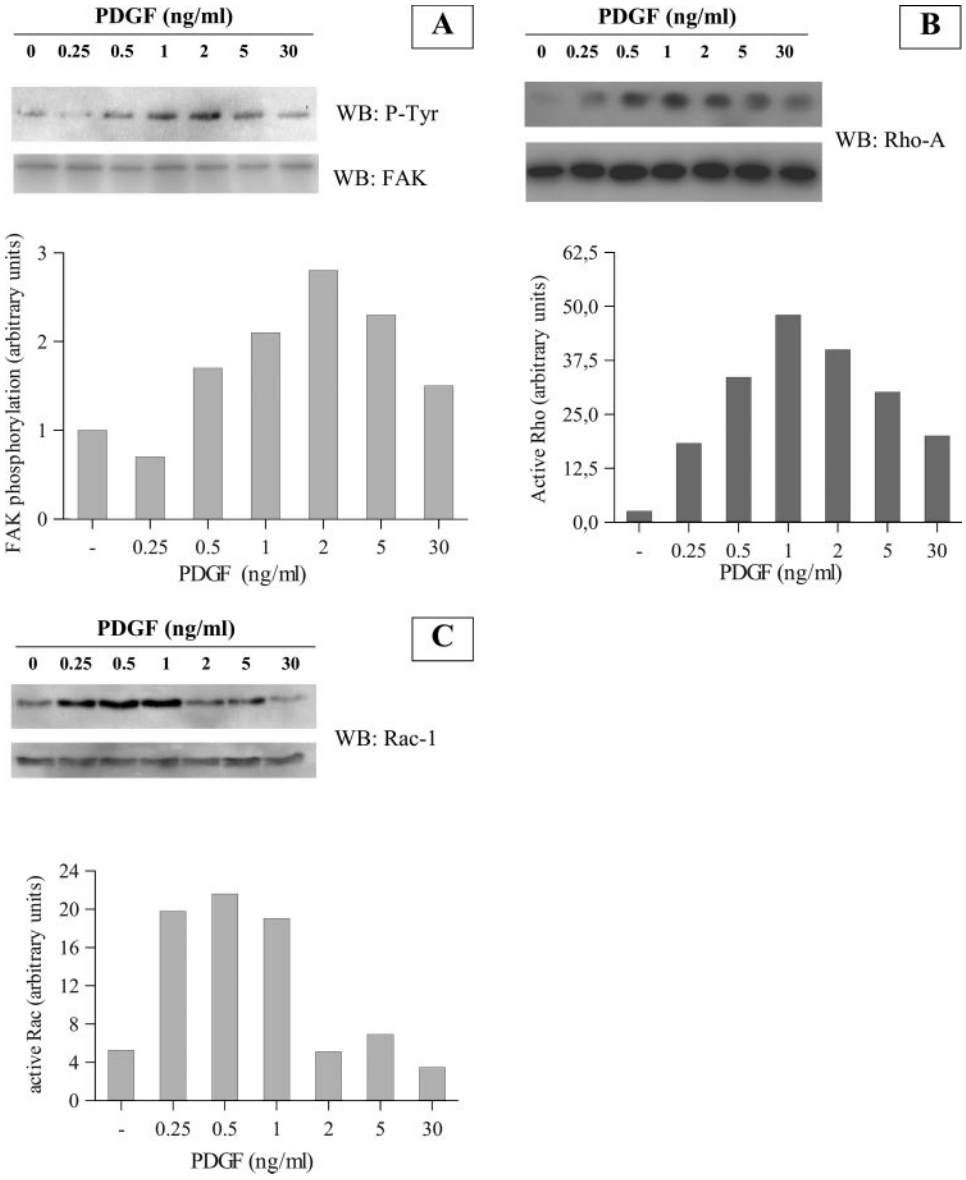

FIGURE 5. *A*, determination of FAK phosphorylation after PDGFR stimulation. NIH3T3 cells were serum-starved for 24 h before stimulation with the indicated concentrations of PDGF for 5 min. FAK was immunoprecipitated from lysates, and anti-phosphotyrosine immunoblotting was performed. The membrane was then stripped and reprobed with anti-FAK antibodies for normalization. The data are representative of three independent experiments. *B*, determination of Rho activity following PDGFR stimulation. NIH3T3 cells were stimulated for 5 min with the indicated concentrations of PDGF 24 h after starvation. The cells were then directly lysed in RIPA buffer, and the lysates were clarified by centrifugation. Lysates were incubated with 10 μg of rhotekin Rho-binding domain-agarose beads, and Rho-GTP was quantified by Western blot (*WB*) analysis. Total RhoA was quantified from lysates for normalization. The histogram represents the ratio between the values of the membranes in *A* and *B*. The data are representative of three independent experiments. *C*, determination of Rac1 activity following PDGFR stimulation. NIH3T3 cells were stimulated for 5 min with the indicated concentrations of PDGF 24 h after starvation. The cells were then directly lysed in RIPA buffer, and the lysates were clarified by centrifugation. Lysates were incubated with 10 μg of PAK-CRIB-GST fusion protein absorbed on glutathione-Sepharose beads, and Rac-GTP was quantified by Western blot analysis. Total Rac1 was quantified from lysates for normalization. The histogram represents the ratio between the values of the membranes in *A* and *B*. The data are representative of three independent experiments.

dose-dependent activation of FAK (Fig. 5*A*) is very different from PDGFR phosphorylation. In fact, maximal FAK phosphorylation was reached at 1–2 ng/ml PDGF stimulation, at which PDGFR phosphorylation was very low, consistent with the evidence that NIH3T3 migration is greater at low PDGF doses.

Rho and Rac belong to the Rho family of small GTPases, and both play a key role in the rearrangement of the actin cytoskeleton related to directional cell migration (20–25). Once activated, these small G proteins are able to recruit intracellular effectors that induce cellular responses, such as protrusion of filopodia (Rac) or lamellipodia (Cdc42) at the leading edge of the cells or events linked to myosin-mediated contractility (Rho), which helps in the retraction of the trailing edge. Rho and Rac activation as a function of PDGF dose stimulation showed a maximum at 1–2 and 0.25–1 ng/ml, respectively. Once again, the time course of Rho/Rac activation did not follow that of PDGFR, in keeping with the evidence that only low PDGF doses are able to induce cell migration (Fig. 5, *B* and *C*). To confirm the role of Rho and Rac activation in low dose PDGF-BB-induced cell migration, we performed the wound healing assay in the presence of both the Rac1 inhibitor NSC23766 (26–28) and the ROCK inhibitor Y-27632 (29). Fig. 6 show that both Rac1 and ROCK inhibitors were able to reduce PDGF-induced migration. In conclusion, low PDGF concentrations (<5 ng/ml) induce cell migration through the activation of pathways such as Rho, Rac, and FAK devoted to cytoskeleton rearrangement, whereas proliferative pathways such as Ras/ERK and PI3K/Akt are not significantly activated. On the other hand, high PDGF concentrations (>5 ng/ml) are essentially pro-mitotic, and consequently, Rho, Rac, and FAK are down-regulated, whereas pathways involved in cell cycle progression are highly stimulated.

PDGF Dose-dependent PDGFR Endocytotic Route—What is the mechanism through which PDGF concentration can determine the cell decision to proliferate or migrate? The answer could reside either in a "qualitative" difference of the single PDGFR molecule depending on the dose of ligand or in a "quantitative" difference. In the first hypothesis, a low dose of PDGF elicits the phosphorylation of a subset of PDGFR tyrosines different from those induced by a high dose of PDGF. This qualitative difference at the level of PDGFR could explain the activation of distinct pathways and hence the different phenotypic outputs. In

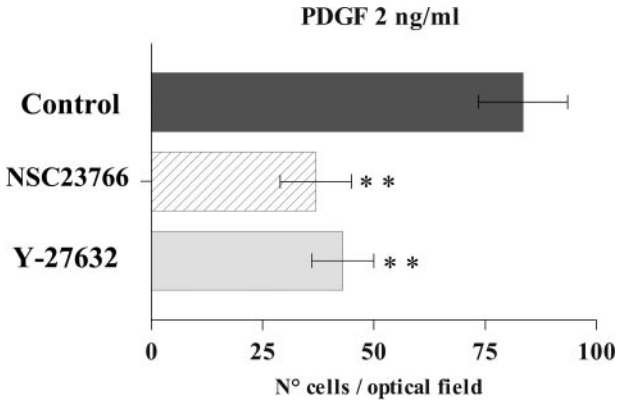

FIGURE 6. **Effects of Rac1 and ROCK inhibitors on NIH3T3 migration.** The wound healing assay was performed on NIH3T3 cells stimulated with 2 ng/ml PDGF as described under "Materials and Methods" in the presence of 10 μM Y-27632 (ROCK inhibitor) or 50 μM NSC23766 (Rac1 inhibitor). The mean migrated cell number ± S.E. was calculated from at least 15 randomly chosen optical fields. The results are representative of three independent experiments. **, $p < 0.001$ *versus* 2 ng/ml PDGF.

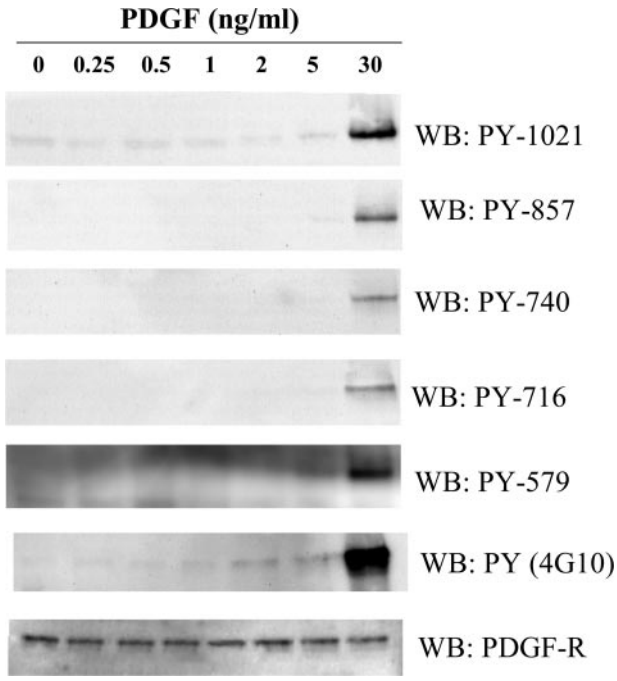

FIGURE 7. **Analysis of PDGFR site-specific phosphorylation.** NIH3T3 cells were stimulated for 5 min with the indicated concentrations of PDGF 24 h after starvation. The cells were then directly lysed in sample buffer, and lysates were used for Western blot (*WB*) analysis with various anti-phospho-PDGFR-specific antibodies and with anti-phosphotyrosine antibodies (4G10) to detect the overall PDGFR phosphorylation level. The data are representative of three independent experiments.

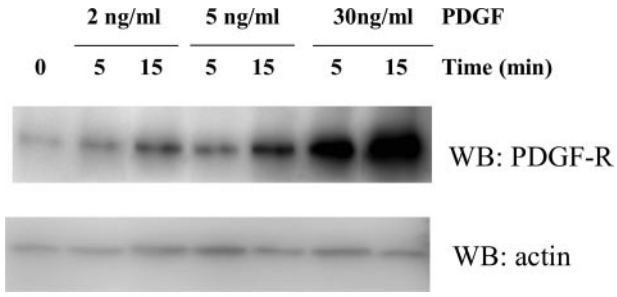

FIGURE 8. **Analysis of endosomal PDGFR after PDGF treatment.** NIH3T3 cells were treated as described under "Materials and Methods" to determine the amount of endosomal PDGFR at the indicated times after stimulation with 2, 5, or 30 ng/ml PDGF. The biotinylated proteins precipitated with streptavidin-agarose resin were subjected to Western blot (*WB*) analysis with anti-PDGFR antibodies. The data are representative of three independent experiments.

the second hypothesis, the tyrosines that are phosphorylated in response to PDGFR stimulation are the same irrespective of the PDGF concentration, so the different cellular behavior as a function of the stimulation dose resides in the number of the activated receptors. To verify the qualitative hypothesis, we analyzed the PDGF dose-dependent activation of five PDGFR tyrosines that recruit important downstream signaling molecules such as PI3K (Tyr^{740}), Src (Tyr^{579}), Grb2 (Tyr^{716}), phospholipase γ1 (Tyr^{1021}), and Tyr^{857}, which are involved in PDGF kinase activation (3). The results show that there were no differences in the phosphorylation of these tyrosines as a function of PDGF concentration (Fig. 7), ruling out the possibility that the differential activation of downstream pathways relies on the tyrosine phosphorylation pattern.

One of the consequences of PDGFR activation is its internalization. Fig. 8 shows that high PDGF concentrations led to a higher PDGFR internalization rate than low doses. This is a quantitative difference because it does not depend on the state of the single PDGFR molecule but on the different number of activated receptors. This result is in agreement with Fig. 1, which shows an ~80% down-regulation of PDGFR expression 1 h after stimulation with 30 ng/ml PDGF, whereas we did not observe a similar effect at low dose stimulation. In fact, to undergo proteasomal/lysosomal degradation, PDGFR has to be internalized (30–32), and high PDGF doses were able to induce a higher PDGFR internalization rate than low doses (Fig. 8). Recently, Sigismund *et al.* (33) demonstrated that the epidermal growth factor receptor (EGFR) at a low ligand dose follows exclusively a CME pathway, whereas at a high ligand dose, EGFR internalization proceeds also through RME. To study the relevance of these two kinds of endocytotic routes at high and low PDGF doses and their relative effects on NIH3T3 cellular behavior, we used two drugs, filipin (0.25 μg/ml) and nystatin (12.5 μg/ml), which preferentially interfere with non-CME-type internalization (33, 34), and siRNA to silence the expression of dynamin-2, a GTPase involved mainly in CME (34). In the latter case, we obtained a 50–60% expression reduction 3 days after transfection with respect to NIH3T3 cells treated with unrelated siRNA (data not shown). Fig. 9*A* shows that, in cells stimulated with low PDGF concentrations, the treatment with dynamin-2 siRNA strongly inhibited PDGF-induced wound repair, suggesting a key role of CME in cell migration. Interestingly, cells treated with RME inhibitors induced increased cell migration compared with control cells, suggesting that inhibiting RME could redirect PDGFR to other endocytotic routes (*i.e.* CME) that are linked to cell-related migration signaling.

In a second set of experiments, we measured cell proliferation at high PDGF concentrations in cells treated with filipin/nystatin and/or dynamin-2 siRNA. Fig. 9*B* shows that the inhibition of RME led to a significant inhibition of cell proliferation, whereas NIH3T3 cells treated with dynamin-2 siRNA (hence inhibiting CME) showed a great increase in cell proliferation

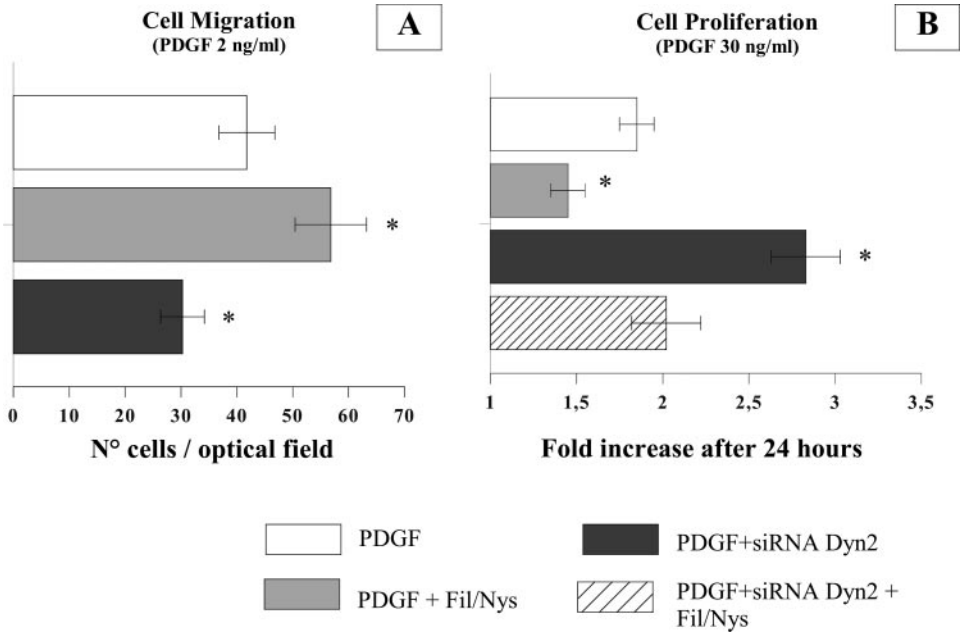

FIGURE 9. *A*, wound healing assay performed on dynamin-2 siRNA-transfected or filipin/nystatin-treated NIH3T3 cells. 24 h after starvation, a wound was produced on the cell layer using a pipette tip. The cells were then stimulated with 2 ng/ml PDGF. 24 h after wounding, the migrated cells in the grid area were counted. The mean migrated cell number ± S.E. was calculated from at least 15 randomly chosen optical fields. The results are representative of three independent experiments. *, $p < 0.005$ *versus* 2 ng/ml PDGF. *B*, NIH3T3 cell proliferation after 30 ng/ml PDGF stimulation. NIH3T3 cells treated with dynamin-2 (*Dyn2*) siRNA for 3 days and/or with filipin/nystatin (*Fil/Nys*) for 1 h before stimulation were starved for 24 h and then stimulated with 30 ng/ml PDGF. After 24 h, cell proliferation was assessed as described under "Materials and Methods." *, $p < 0.005$ *versus* 30 ng/ml PDGF.

compared with control cells. These data indicate that RME is important for PDGF mitogenesis induction and that the proliferative effect of CME inhibition could be due to the redirection of PDGFR molecules to the pro-proliferative RME pathway. This hypothesis is confirmed by the fact that NIH3T3 cells treated with both dynamin-2 siRNA and RME inhibitors behaved similarly to the control cells, pointing to RME as responsible for the "extra" proliferation of dynamin-2 siRNA-transfected cells.

DISCUSSION

PDGFR is a transmembrane receptor whose activation play an essential role in promoting and controlling many aspects of cell physiology such as mitosis, migration, and metabolism, as well as differentiation. In particular, two of these cellular responses, proliferation and migration, appear to be mutually exclusive for an individual cell at a given time. To clarify this apparent contradiction, we developed a very simple model in which the phenotypic output of a given cell depends essentially on the concentration of PDGF.

First, we studied the ligand dose and the time and dose-dependent activation of PDGFR (Fig. 1) in relation to the phenotypic outcome induced in NIH3T3 cells. Our results show that, although PDGFR phosphorylation increases almost linearly as a function of the PDGF dose, the cellular response is not linear at all. Low PDGF concentrations (<2 ng/ml) were totally unable to induce cell proliferation (Fig. 2) but were more efficient in promoting cell migration than the higher doses both in wound healing experiments (Fig. 3*A*) and in the two-dimensional migration and proliferation assay tests (Fig. 3, *B* and *C*). Conversely, a high PDGF concentration (30 ng/ml) was able to induce a strong proliferating stimulus (Fig. 2) but had a minor effect on promoting cell migration compared with the lower doses (Fig. 3). The transition between these two cellular phenotypic responses takes place without solution of continuity being, for example, 5 ng/ml PDGF able to induce both mitogenesis and migration. A likely explanation of this effect would be that, in these conditions, two different subsets of the cell population make different behavioral decisions.

Next, we analyzed some intracellular signaling pathways triggered by PDGFR activation. We found that of the two pathways linked with cell cycle progression examined, one, ERK (Fig. 4*A*), follows the same dose-dependent activation as PDGFR itself, whereas the other, PI3K/Akt (Fig. 4*B*), begins to be detectably active even at low doses (2–5 ng/ml). An explanation of this phenomenon may reside in the fact that not only Akt is involved in mitosis, but its activation is mandatory for cell survival, and hence its effects must be present also at low PDGF concentrations. We then examined three downstream PDGFR mediators that are strictly linked with cytoskeleton remodeling during cell migration: FAK, Rho, and Rac1 (Figs. 5, *A–C*; and 6). The activation of these three proteins is marked at low PDGF concentrations (in conditions permissive for cell migration), whereas at high PDGF concentrations, at which mitogenic signaling prevails, their functional activation is lowered.

At this point, it is clear that PDGFR induces different and, for many aspects, opposite cellular responses through differential activation of intracellular signaling pathways, sensing the environmental concentration of its ligand. To explain this outcome, we developed two hypotheses. The qualitative hypothesis states that PDGFR phosphorylation is differentially stimulated by different PDGF doses, activating different subsets of signaling pathways. The quantitative hypothesis predicts that PDGFR activation is an all-or-none phenomenon so that every individual dimer of activated receptor is phosphorylated in the same way (*i.e.* has an identical tyrosine phosphorylation pattern) irrespective of the environmental ligand concentration. In the latter case, the PDGF dose simply influences the number of activated receptors. Our data rule out the first hypothesis because we could not measure a differential phosphorylation state of the five diverse PDGFR tyrosines as a function of ligand concentration (Fig. 7).

One of the consequences of activation of receptor tyrosine kinases is their internalization. Not only is this event linked to their ubiquitination and proteasomal degradation, but it is well

established that endosomal receptor tyrosine kinases play an important role in signal transduction (35, 36). In particular, regarding PDGFR, Wang *et al.* (5) showed that endosomal PDGFR signaling is sufficient to activate the major signaling pathways that allow cell proliferation. Herein, we confirmed that it is not only sufficient but also necessary. First, we assessed that the PDGFR internalization rate depends on the concentration of the ligand (Fig. 8). PDGF at 30 ng/ml induces much more PDGFR endocytosis compared with 1 or 5 ng/ml. Sigismund *et al.* (33) observed that EGFR endocytosis proceeds through two different pathways: at low ligand stimulation doses, EGFR internalization depends exclusively on the CME pathway, whereas at high doses, EGFR endocytosis proceeds also through RME. We interfered with both CME (lowering the dynamin-2 expression level) and RME (using two pharmacologic inhibitors, filipin and nystatin) and studied the cellular behavior at low and high PDGF doses. Our data suggest that there is a balance (which depends on ligand concentrations) between these two kind of PDGF endocytotic routes that determines the cellular response. In fact, we found that, at low PDGF concentrations, which are exclusively permissive for cell migration, CME does play a functional role in this phenomenon because in cells in which dynamin-2 was silenced, cell migration was inhibited (Fig. 9*A*). Interestingly, cells treated with filipin and nystatin showed a significant increase in cell migration, supporting the idea that, in the presence of RME inhibition, PDGFR CME is strengthen, thus leading to higher cell motility.

On the other hand, at high PDGF concentrations, at which cell proliferation is the prevalent effect, RME inhibition led to a corresponding inhibition of cell proliferation (Fig. 9*B*), indicating that RME represents a signal transduction pathway that is essential for PDGFR-mediated mitogenesis. Consequently, RME-dependent PDGFR degradation represents merely a consequence and not the aim of the RME route. In addition, in cells stimulated with high PDGF concentrations, inhibition of CME in dynamin siRNA-treated cells led to a great increase in cell proliferation compared with control cells (Fig. 9*B*). Similar to what was discussed above, the inhibition of CME could induce a shift in the PDGFR internalization route toward RME, thus leading to a stronger proliferative response compared with control cells. This "balance and shift" hypothesis is reinforced by the fact that dynamin-2 siRNA-transfected cells treated with filipin/nystatin show a proliferation response similar to control cell, indicating that RME is responsible for the extra proliferative signaling of CME-inhibited cells.

In conclusion, PDGFR appears to have two distinct functions depending on the environmental ligand concentration. Similar to EGF (33), low PDGF doses induced exclusively CME that was strongly involved in cell migration but was not essential for cell proliferation (Fig. 9*A*). Under these conditions, PDGFR acts like a sensor on the cell surface guiding cell migration, and CME could play an essential role in regenerating free PDGFR on the surface that is needed to sense the PDGF gradient. Notably, low PDGF doses did not lead, at least within 1 h, to appreciable PDGFR down-regulation (Fig. 1), which was instead very high when cells were stimulated with high doses, strengthening the hypothesis of a sensor-like function for PDGFR in these conditions.

At high PDGF doses, PDGFR internalization is mediated also by RME, and this endocytic route is not only sufficient (5) but also necessary for PDGF-induced cell proliferation (Fig. 9*A*). Therefore, we propose that the dual "face" of PDGFR signaling depends on the environmental concentration of PDGF sensed by each target cell. Low PDGF concentrations are able to induce directional migration toward the ligand source. When the cell, migrating along the increasing gradient, finds the minimal PDGF concentration that is sufficient to induce proliferation, it stops moving and enters mitosis. This model can be easily applied to a variety of physiologic and pathologic situations such as wound healing, angiogenesis, and metastasis and can likely be extended to describe the behavior of many other receptor tyrosine kinases.

REFERENCES

1. Schlessinger, J. (2000) *Cell* **103,** 211–225
2. Hoch, R. V., and Soriano, P. (2003) *Development* (*Camb.*) **130,** 4769–4784
3. Heldin, C. H., and Westermark, B. (1999) *Physiol. Rev.* **79,** 1283–1316
4. Tallquist, M., and Kazlauskas, A. (2004) *Cytokine Growth Factor Rev.* **15,** 205–213
5. Wang, Y., Pennock, S. D., Chen, X., Kazlauskas, A., and Wang, Z. (2004) *J. Biol. Chem.* **279,** 8038–8046
6. Rönnstrand, L., and Heldin, C. H. (2001) *Int. J. Cancer* **91,** 757–762
7. Parenti, A., Donnini, S., Morbidelli, L., Granger, H. J., and Ziche, M. (1997) *Br. J. Pharmacol.* **119,** 619–621
8. Roberts, M., Barry, S., Woods, A., van der Sluijs, P., and Norman, J. (2001) *Curr. Biol.* **11,** 1392–1402
9. Brunet, A., Roux, D., Lenormand, P., Dowd, S., Keyse, S., and Pouysségur, J. (1999) *EMBO J.* **18,** 664–674
10. Murphy, L. O., and Blenis, J. (2006) *Trends Biochem. Sci.* **31,** 268–275
11. Collado, M., Medema, R. H., Garcia-Cao, I., Dubuisson, M. L., Barradas, M., Glassford, J., Rivas, C., Burgering, B. M., Serrano, M., and Lam, E. W. (2000) *J. Biol. Chem.* **275,** 21960–21968
12. Medema, R. H., Kops, G. J., Bos, J. L., and Burgering, B. M. (2000) *Nature* **404,** 782–787
13. Brazil, D. P., Yang, Z. Z., and Hemming's, B. A. (2004) *Trends Biochem. Sci.* **29,** 233–242
14. Liang, J., Zubovitz, J., Petrocelli, T., Kotchetkov, R., Connor, M. K., Han, K., Lee, J. H., Ciarallo, S., Catzavelos, C., Beniston, R., Franssen, E., and Slingerland, J. M. (2002) *Nat. Med.* **8,** 1153–1160
15. Franke, T. F., Kaplan, D. R., and Cantley, L. C. (1997) *Cell* **88,** 435–437
16. Ilić, D., Furuta, Y., Kanazawa, S., Takeda, N., Sobue, K., Nakatsuji, N., Nomura, S., Fujimoto, J., Okada, M., and Yamamoto, T. (1995) *Nature* **377,** 539–544
17. Ren, X. D., Kiosses, W. B., Sieg, D. J., Otey, C. A., Schlaepfer, D. D., and Schwartz, M. A. (2000) *J. Cell Sci.* **113,** 3673–3678
18. Mitra, S. K., Hanson, D. A., and Schlaepfer, D. D. (2005) *Nat. Rev. Mol. Cell Biol.* **6,** 56–68
19. McLean, G. W., Carragher, N. O., Avizienyte, E., Evans, J., Brunton, V. G., and Frame, M. C. (2005) *Nat. Rev. Cancer* **5,** 505–515
20. Raftopoulou, M., and Hall, A. (2003) *Dev. Biol.* **265,** 23–32
21. Yamazaki, D., Kurisu, S., and Takenawa, T. (2005) *Cancer Sci.* **96,** 379–386
22. Fukata, M., Nakagawa, M., and Kaibuchi, K. (2003) *Curr. Opin. Cell Biol.* **15,** 590–597
23. Nobes, C. D., and Hall, A. (1999) *J. Cell Biol.* **144,** 1235–1244
24. Xu, J., Wang, F., Van Keymeulen, A., Herzmark, P., Straight, A., Kelly, K., Takuwa, Y., Sugimoto, N., Mitchison, T., and Bourne, H. R. (2003) *Cell* **114,** 201–214
25. Even-Ram, S., and Yamada, K. M. (2005) *Curr. Opin. Cell Biol.* **17,** 524–532

26. Désiré, L., Bourdin, J., Loiseau, N., Peillon, H., Picard, V., De Oliveira, C., Bachelot, F., Leblond, B., Taverne, T., Beausoleil, E., Lacombe, S., Drouin, D., and Schweighoffer, F. (2005) *J. Biol. Chem.* **280,** 37516–37525
27. Gao, Y., Dickerson, J. B., Guo, F., Zheng, J., and Zheng, Y. (2004) *Proc. Natl. Acad. Sci. U. S. A.* **101,** 7618–7623
28. Birukova, A. A., Alekseeva, E., Mikaelyan, A., and Birukov, K. G. (2007) *FASEB J.* **21,** 2776–2786
29. Narumiya, S., Ishizaki, T., and Uehata, M. (2001) *Methods Enzymol.* **325,** 273–284
30. Sorkin, A., Westermark, B., Heldin, C. H., and Claesson-Welsh, L. (1991) *J. Cell Biol.* **112,** 469–478
31. Mori, S., Heldin, C. H., and Claesson-Welsh, L. (1992) *J. Biol. Chem.* **267,** 6429–6434
32. Mori, S., Rönnstrand, L., Claesson-Welsh, L., and Heldin, C. H. (1994) *J. Biol. Chem.* **269,** 4917–4921
33. Sigismund, S., Woelk, T., Puri, C., Maspero, E., Tacchetti, C., Transidico, P., Di Fiore, P. P., and Polo, S. (2005) *Proc. Natl. Acad. Sci. U. S. A.* **102,** 2760–2765
34. Pelkmans, L., Püntener, D., and Helenius, A. (2002) *Science* **296,** 535–539
35. Miaczynska, M., Pelkmans, L., and Zerial, M. (2004) *Curr. Opin. Cell Biol.* **16,** 400–406
36. Polo, S., and Di Fiore, P. P. (2006) *Cell* **124,** 897–900

Proliferation *Versus* Migration in Platelet-derived Growth Factor Signaling: THE KEY ROLE OF ENDOCYTOSIS

Alina De Donatis, Giusy Comito, Francesca Buricchi, Maria C. Vinci, Astrid Parenti, Anna Caselli, Guido Camici, Giampaolo Manao, Giampietro Ramponi and Paolo Cirri

J. Biol. Chem. 2008, 283:19948-19956.
doi: 10.1074/jbc.M709428200 originally published online May 21, 2008
